

Mean Free Path of Electrons and Magnetomorphic Effects in Small Single Crystals of Gallium*

M. YAQUB† AND J. F. COCHRAN

*Department of Physics and The Center for Materials Science and Engineering,
Massachusetts Institute of Technology, Cambridge, Massachusetts*

(Received 6 August 1964)

The variation of electrical resistivity of 99.9999%-pure gallium has been investigated as a function of size in oriented single crystals for current flow along the C axis. The crystals were in the form of wires of square cross section and their dimensions varied from 1 to 0.1 mm. Analysis of the data based on the free-electron model, assuming diffuse scattering at the boundaries, yields a value of $8.11 \times 10^{-11} \Omega\text{-cm}^2$ for $(\rho_b l_b)_{C \text{ axis}}$ and indicates that at 0°K the mean free path of the charge carriers in the bulk metal is considerably in excess of 1 cm. The temperature dependence of the size effect seems to be in fair agreement with a theory due to Blatt and Satz. Within the accuracy of our measurements the ideal bulk resistivity at low temperatures varies as T^2 , indicating that the electron-electron collisions may be contributing to the resistive processes. For low values of a longitudinal magnetic field, all the crystals showed a large decrease in resistance followed by an increase due to bulk magnetoresistance, both at 4.2° and at 1.2°K. For the same two temperatures these crystals also displayed a rather large magnetoresistance in transverse magnetic fields. Magnetomorphic effects for transverse fields were evidenced by the fact that the field dependence of magnetoresistance was less than quadratic for all crystals until the cyclotron radius of the charge carriers acquired a value much smaller than the cross-sectional dimensions of the specimens. The resistance of all the crystals was found to be a complicated function of the measuring current. Calculations based on certain simplifying assumptions show that for thin wires in which boundary scattering is predominant, the resistance decreases monotonically as a function of the current and is due to the trapping of the charge carriers in the magnetic field generated by the current. The details of the experimental curves can be reproduced reasonably well if the fall in resistance due to the trapped particles is superimposed on the magnetoresistance caused by the self field.

I. INTRODUCTION

FOR a free-electron gas the resistivity of a metal in bulk can be written as

$$\rho_b = (\bar{P}/ne^2)(1/l_b), \quad (1.1)$$

where n is the number of electrons per unit volume, e the charge, \bar{P} their average momentum, and l_b the mean free path. From Eq. (1.1), it is clear that $\rho_b l_b$ is an intrinsic quantity of the metal whose determination by experimental means is of great interest. It not only serves as a check on the electronic theories, but also provides valuable information about the electronic structure of the metals and enables us to determine the mean free path of their charge carriers. $\rho_b l_b$ can be obtained from the resistivity of a metal provided that a specimen can be prepared in which the mean free path of the charge carriers is known. This can be achieved by using specimens in the form of wires or films which are so thin that the scattering of electrons at the surfaces of the specimen, a process which is normally negligible in comparison with electron scattering within the volume of the metal, now plays a dominant role. The resistivity of the metal is increased above its value in the bulk and from this increase one can determine the ratio of the bulk free path to the thickness of the film or the diameter of the wire. This was first realized by J. J. Thomson¹ in 1901 who gave an approximate expression for the

increase in resistance of a thin film. Thomson's ideas were confirmed by Patterson² who measured the resistance of thin Bi films. The value of l_b , 10^{-4} cm, obtained from these experiments was considered inconceivably high in those days, and therefore further experiments of this nature were abandoned.

Interest in the determination of mean free paths by means of the size effect was revived in the early thirties when quantum mechanics and the Pauli exclusion principle predicted a high degeneracy for a gas of electrons in a metal. For a Fermi gas, Eq. (1.1) becomes

$$\rho_b l_b = P_f / ne^2, \quad (1.2)$$

where P_f now stands for the momentum of an electron at the Fermi surface. A high degeneracy means that the variation of n in Eq. (1.2), and hence of $\rho_b l_b$ with temperature, is negligible. The change of resistivity as a function of temperature in a metal would therefore be a direct measure of the change in the mean free path of its electrons. In particular, it was realized that at very low temperatures, the electrons would be scattered mainly by impurities so that the effect of surface scattering on the resistivity should be readily observable in small specimens prepared from very pure metals.

Until recently, all size-effect measurements showed that commercially available "pure" metals had a high concentration of impurities, and therefore in order to see the effects of boundary scattering dimensions of the order of 10^{-3} cm were required. Specimens of this size could not be obtained in the form of single crystals. Evaporated films or extruded wires on which most of

* Work supported in part by ARPA and in part by the U. S. Army Signal Corps, the U. S. Air Force Office of Scientific Research, and the U. S. Office of Naval Research.

† Present address: Physics Department, Ohio State University, Columbus, Ohio.

¹ J. J. Thomson, Proc. Cambridge Phil. Soc. **11**, 120 (1901).

² J. A. Patterson, Proc. Cambridge Phil. Soc. **11**, 118 (1901).

the experiments were conducted were always polycrystalline. It was also doubtful whether their behavior was the same as that of the bulk metal. Recently, however, size-effect measurements have received further impetus because metals of a much greater degree of purity have now become available. At low temperatures, the mean free path of electrons in these metals is so large that the effect of boundary scattering can be detected in single crystal wires of 1 mm diam. Recent measurements by Alexandrov³ have revealed mean free paths of 1–2 mm in single crystals of Al, In, Pb, Sn, Zn, Cd, and Bi at 1.5°K. Of course, once having determined the quantity $\rho_b l_b$ from size-effect measurements on very pure metals, it then becomes possible to use the bulk resistivity as a tool for studying the effect of impurities, lattice imperfections, and thermal agitation upon the carrier mean free path.

It is an empirical fact that the results of size-effect measurements on cylindrical wires of diameter d can be represented by

$$\rho_a(T) = \rho_b(T) + (A/d), \quad (1.3)$$

where $\rho_a(T)$ is the resistivity of the wire and $\rho_b(T)$ the bulk resistivity. The term A/d , where A is a temperature dependent parameter, characteristic of a given metal, takes into account the additional contribution to resistance by the surface scattering of electrons. Tisza⁴ was the first to give a simple explanation of Eq. (1.3) in terms of the mean free paths characterized by different scattering mechanisms. Assuming that they are additive, we would have

$$1/l_a = 1/l_b + 1/l_s, \quad (1.4)$$

where l_a is the effective mean free path in the wire, and l_b and l_s are the free paths for the bulk metal and surface scattering, respectively. Now l_s , which must depend on the diameter, can be written as

$$l_s = d/\alpha$$

whence

$$\rho_a = \rho_b l_b / l_a = \rho_b + \alpha(\rho_b l_b / d), \quad (1.5)$$

and this is of the same form as Eq. (1.3). α is a parameter whose value depends on the metal concerned, and whose calculation requires (a) a supposition about the character of the surface scattering, (b) an assumption about the existence of a bulk mean free path, and (c) a knowledge of the geometry of the Fermi surface. The problem of how the electrons are scattered by the surface of a metal is very difficult. Theoretical papers on this question do not go beyond introducing a coefficient of specular reflection p , according to which a fraction p of the incident electrons are reflected specularly whilst the remainder are diffusely scattered in all directions. This is the simplest way of covering the whole range of cases lying between $p=0$ for which the surface is per-

fectly rough and $p=1$ for which it is perfectly smooth. The wavelength of electrons at the Fermi surface of most metals is of the order of a few angstroms, whereas even in optically polished surfaces the asperities are a few thousand angstroms. Under such conditions it is difficult to imagine how a surface could appear smooth to an electron moving with the Fermi velocity. It is therefore generally assumed that the scattering by a surface is diffuse and $p=0$. Only for Bi is there evidence that the carriers may be specularly reflected, at least in part.⁵

The problem of the existence of a mean free path is extremely complicated and can be justified only under certain restricted conditions. Although a free path can always be defined for scattering by randomly distributed impurity atoms, its concept for scattering by lattice vibrations is strictly valid only when temperatures are higher than the Debye temperature and the high-frequency modes are fully excited. For the purpose of electrical conductivity, however, it is generally considered reasonable to assume that a mean free path can be defined for all temperatures and that the temperature variation of the path is the same as that of the electrical conductivity. On account of the complications involved, the possible variations of the free path as a function of its position on the Fermi surface has always been ignored in all theoretical calculations of size effects.

A detailed analysis of the conductivity of small cylindrical wires has been worked out by Dingle⁶ and by Chambers⁷ for an isotropic metal assuming a spherical Fermi surface. According to these authors the resistivity for a wire of diameter d is given by

$$\rho_a = \rho_b + \frac{3}{4}(1-p)(\rho_b l_b / d) \quad \text{when } d/l_b \gg 1 \quad (1.6)$$

and

$$\rho_a = [(1-p)/(1+p)](\rho_b l_b / d) \quad \text{when } d/l_b \ll 1. \quad (1.7)$$

MacDonald and Sarginson⁸ have shown that Eq. (1.6) also holds for a wire of square cross section if d represents the side of the wire, but Eq. (1.7) has to be modified to

$$\rho_a = \left(\frac{1-p}{1+p} \right) \frac{\rho_b l_b}{d} \times \frac{1}{1.116} \quad \text{for } \frac{d}{l_b} \ll 1. \quad (1.8)$$

A theory of surface scattering for circular wires assuming an arbitrary Fermi surface and diffuse scattering has been formulated by Alexandrov and Kaganov⁹ and by Bate, Martin, and Hille,¹⁰ but has not been

⁵ A. N. Friedman and S. H. Koenig, IBM J. Res. Develop. 4, 158 (1960).

⁶ R. B. Dingle, Proc. Roy. Soc. (London) A201, 545 (1950).

⁷ R. G. Chambers, Proc. Roy. Soc. (London) A202, 378 (1950).

⁸ D. K. C. MacDonald and K. Sarginson, Proc. Roy. Soc. (London), A203, 223 (1950).

⁹ B. N. Alexandrov and M. I. Kaganov, Zh. Eksperim. i Teor. Fiz. 41, 1333 (1961) [English transl.: Soviet Phys.—JETP 14, 948 (1962)].

¹⁰ R. T. Bate, B. Martin, and P. F. Hille, Phys. Rev. 131, 1482 (1963).

³ B. N. Alexandrov, Zh. Eksperim. i Teor. Fiz. 43, 339 (1962) [English transl.: Soviet Phys.—JETP 16, 286 (1963)].

⁴ L. Tisza, Naturwiss. 19, 86 (1931).

worked out in a form which could be applied to a real metal.

The above discussion clearly indicates that Eq. (1.5) is still the most convenient expression for comparison with observations. For the general assumption of a spherical Fermi surface and diffuse scattering, it is identical with Eq. (1.3) which is invariably employed to represent the experimental results. The resulting straight line whose slope is $\rho_b l_b$ intersects the resistivity axis at ρ_b ; it is thus possible to obtain l_b .

Since $\rho_b l_b$ is invariant for a given metal, the slope of this straight line should be independent of the temperature at which the observations are taken. In actual practice, however, this is not so. It turns out that the slope steadily increases as a function of the temperature. This was first noticed in Hg and Sn by Andrew¹¹ and subsequently in indium by Olsen,¹² who suggested the following simple explanation.

At very low temperatures the normal electron phonon scattering is essentially a small angle event of the order of T/Θ_D where Θ_D is the Debye temperature. In order to remove the momentum given to the electrons by the electric field a large number of such collisions may be necessary. In the bulk metal, therefore, this would not be very effective in causing resistance. In thin specimens, on the other hand, it requires only a few collisions to deflect the electrons to the surface where diffuse scattering can cause an increase in resistance. As a result, the decrease in resistivity as a function of temperature is less rapid in small specimens than in the bulk metal. This mechanism has been treated theoretically by Luthi and Wyder,¹³ Blatt and Satz,¹⁴ and Azbel' and Gurzhi.¹⁵ Blatt and Satz derive an explicit mathematical relation which is easy to compare with experiments. Assuming Mathiessen's rule to be true for different scattering mechanisms, they give the following expression for the size and temperature-dependent resistivity of a thin wire.

$$\rho_d(T) = \rho_r + \rho_i(T) + (A/d) + [8\pi f \rho_i(T)]^{1/3} \times [(T/\Theta_D)(\rho_b l_b/d)]^{2/3} \text{ for } d/l_i \ll 1. \quad (1.9)$$

In this equation, ρ_r is the residual bulk resistivity, $\rho_i(T)$ is the temperature-dependent bulk resistivity of the ideal metal characterized by a mean free path, l_i , A is the slope of the resistivity as a function of $1/d$ at $T=0^\circ\text{K}$, and Θ_D the Debye temperature. At low temperatures, electron-phonon collisions are by no means the only events responsible for the ideal resistivity $\rho_i(T)$. Contributions due to other processes are possible and these are taken into account by introducing a fraction f in the last term of the equation. One of these

additional processes may be the so-called umklapp or reversal events. If, in a metal, the zone boundary is close to the Fermi surface, then it is also close to its mirror image in the periodically extended zone scheme. Thus, a low-energy phonon with appropriate momentum can bridge the small separation, causing an electron to undergo a Bragg reflection. This is called an umklapp process. Contrary to the normal processes, umklapp processes nearly reverse the direction of the electron's velocity and therefore may play an important role in the temperature-dependent resistance at low temperatures.

The last term of Eq. (1.9) is usually only 5–10% of $\rho_i(T)$, and it is not possible to distinguish between a d^{-1} or $d^{-2/3}$ dependence on the wire diameter for the limited range of d^{-1} (0–100 cm^{-1}) usually used for size-effect measurements. The effect of this term, therefore, is to change the slope of the straight line represented by Eq. (1.5), which now becomes temperature-dependent. It is clear that Eq. (1.9) provides us with a method of determining the ratio of normal events to any other scattering events which may be present. This has been applied to In¹⁴, Hg¹⁴, and Al³, for which the values of f obtained are 0.04, 0.14, and 1, respectively.

In this paper we describe the results of the variation of size on the resistivity of single crystal wires of gallium in which the C axis coincided with the axis of the wire. The results have been analyzed on the basis of the theories outlined above.

Results are also given for the measurements of magnetoresistance of these crystals for longitudinal fields up to a maximum of 1400 G and transverse fields up to 400 G.

In a subsequent paper, similar results for the A - and the B -axis crystals will be discussed. A preliminary account of these measurements has already appeared in print.^{16,17}

II. EXPERIMENTAL DETAILS

Specimen Preparation

The single crystals of gallium were prepared from 99.9999+% pure metal supplied by the Aluminum Company of America, Pittsburgh 19, Pennsylvania. They were in the form of wires with a square cross section, and were grown in Lucite molds by injecting liquid gallium into channels of appropriate size. The potential leads were grown as an integral part of the crystals in order to avoid the strain and damage which might have resulted from later attaching leads of a different metal. Figure 1(a) shows the bottom plate of a typical mold with four spacers which form the necessary channels. In order to obtain a square cross section, the width of the central channel running across the length of the mold was made the same as the thickness of the spacers

¹¹ E. R. Andrew, Proc. Phys. Soc. (London), **A62**, 77 (1949).

¹² J. L. Olsen, Helv. Phys. Acta **31**, 713 (1958).

¹³ B. Luthi and P. Wyder, Helv. Phys. Acta **33**, 667 (1960).

¹⁴ F. J. Blatt and H. G. Satz, Helv. Phys. Acta **33**, 1007 (1960).

¹⁵ M. Ya. Azbel' and R. N. Gurzhi, Zh. Eksperim. i Teor. Fiz. **42**, 1632 (1962). [English transl.: Soviet Phys.—JETP **15**, 1133 (1962)].

¹⁶ M. Yaqub and J. F. Cochran, Phys. Rev. Letters **10**, 390 (1963).

¹⁷ J. F. Cochran and M. Yaqub, Phys. Letters **5**, 307 (1963).

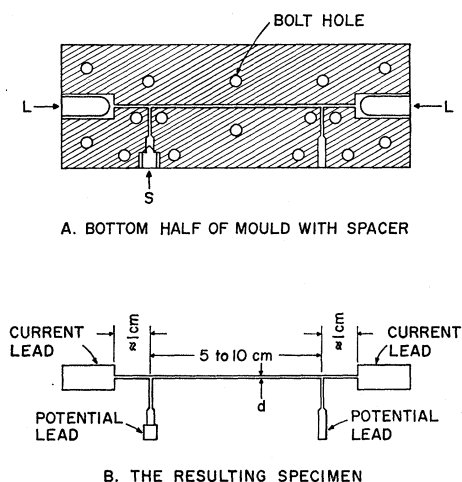


FIG. 1. The construction of the mold and the resulting specimen.

by placing a wire of the right diameter in between the spacers, which were then pressed firmly against the wire. The mold was then completed by placing a second piece of Lucite of the same dimensions as the first on top of the spacers, and was held together by means of bolts passing through both plates. Grooves cut into the lower plate at L on either side provided the crystals with heavy ends which served as terminals for the current leads. A hole, centrally situated with respect to the outer plates, was drilled at S and was just the right size to take the nozzle of a 2-cc hypodermic syringe used to fill the channels. The mold was now dismantled and thoroughly cleaned with distilled water and pure alcohol. It was then reassembled without the wire and filled with molten gallium.

On account of its high purity, the liquid showed no tendency towards solidification several degrees below its melting point, which is 29.8°C . The liquid could therefore be injected at normal room temperatures. After filling the mold, a seed crystal of the desired orientation was carefully placed at one of the ends marked L in Fig. 1(a) and the liquid was made to touch it by pressing on the piston of the syringe. This immediately started the process of solidification, which could be easily watched through the transparent mold because the solid phase appeared darker in color than the liquid. The velocity of growth is controlled by the rate at which the heat of solidification at the phase boundary can be conducted away. For a surrounding temperature of 24°C , it took approximately one hour to grow a typical crystal. The resulting crystal, shown in Fig. 1(b), had a square cross section to within 0.001 cm, with two mirror surfaces where the molten metal was in contact with the Lucite plates, and two matt surfaces where it was against the spacers. The spacers of the first three of the six crystals listed in Table II were of Lucite, and of the remaining three were of paper.

During growth, the liquid-solid boundary had a char-

acteristic shape for the three principal axes of the orthorhombic lattice. For growth along the C axis, the boundary was either a line perpendicular to the direction of growth or an acute angle with its apex projecting into the liquid. For growth along the A axis, the interphase boundary was nearly a right angle, and along the B axis an obtuse angle which appeared nearly supplementary to the acute angle of growth along the C axis. This was of great practical importance in detecting changes of orientation that sometimes occurred during growth and in the initial stages of crystallization, when, by merely looking at the boundary, it could be ascertained whether the crystal had started to grow in the desired orientation or not. When the process of crystallization was completed, the bottom plate of the mold was carefully removed, without disturbing the position of the crystal with respect to the other plate. The orientation of the crystal was then checked with an x-ray back reflection Laue photograph of the heavy current terminals at both ends. The Lucite plates were originally very carefully machined and the central part of the thin crystal was always kept exactly parallel to their edges. The edges thus acted as reference planes for determining the orientation of the crystal. Crystals whose wires did not coincide with the crystallographic axes to within a degree were rejected. In Fig. 2 are shown back reflection photographs of three typical crystals used in the measurements. The x-ray beam in (a), (b), and (c) is parallel to the A, B, and C axis, respectively. The photographs are reproduced here in order to show the sharpness of the spots which indicate a high degree of perfection of the crystals, and also to label the different axes unambiguously. There seems to be some confusion in the literature about labeling the A and the B axis (Barrett¹⁸).

The crystal was then transferred from the rest of the mold and mounted on a single-crystal rectangular plate of gallium ($10\text{ cm} \times 2.5\text{ cm} \times 2\text{ mm}$) in such a way that the corresponding crystallographic axes in the specimen and the plate were parallel. They were electrically insulated from each other by a layer of thin tissue paper held in position by a thin coating of GE-7031 varnish. This procedure guaranteed the specimen to be strain free on cooling to helium temperatures. Current was led to the specimen by means of thick copper wires which were soldered to the heavy ends.

In order to calculate the resistivities, the average cross-sectional area of the crystals had to be determined accurately. It was computed, after all the electrical measurements had been made, by weighing a known length of the crystal to the nearest hundredth of a milligram and using a value of 5.907 g/cc as the density¹⁹ of the metal at 20°C . Dimensions thus obtained agreed to within a few percent with the diam-

¹⁸ C. S. Barrett (private communication).

¹⁹ T. W. Richards and S. Boyer, *J. Am. Chem. Soc.* **43**, 274 (1921).

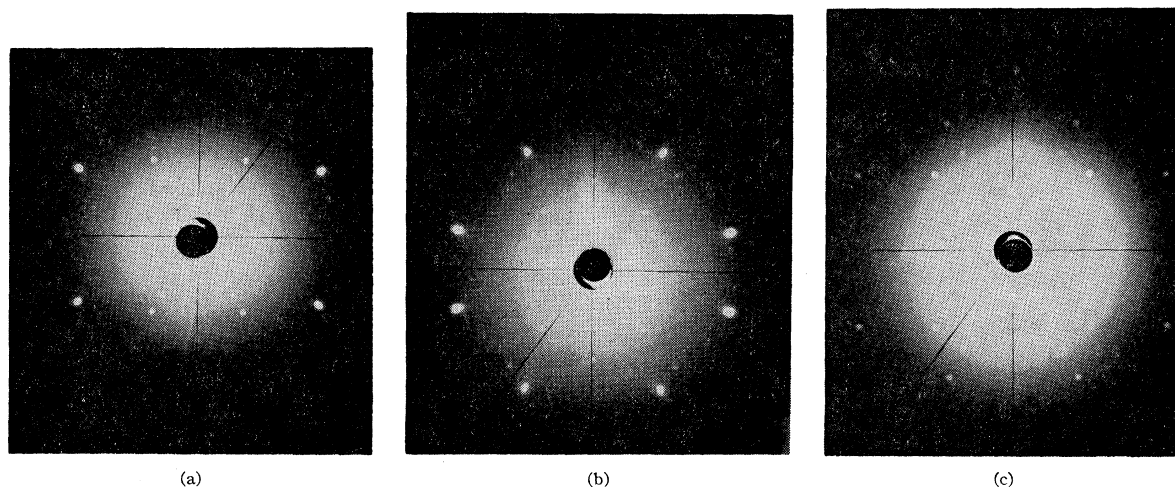


FIG. 2. Laue back reflection photographs of three oriented crystals. (a) Incident x-ray beam parallel to the *A* axis. (b) Incident x-ray beam parallel to the *B* axis. (c) Incident x-ray beam parallel to the *C* axis.

eter of the wire used in assembling the mould. In calculating the resistivities at different temperatures, appropriate corrections for changes in lengths were applied using Powell's²⁰ thermal expansion data between 293° and 77°K, and Barrett's (see Ref. 42) x-ray values of the lattice constants at 2.35° and at 77°K (see Table I).

Resistance Measurements

Conventional techniques were employed to measure the resistance. The current was supplied from heavy-duty car batteries, and was maintained constant to 0.1% by means of a homemade regulator designed to operate over a range of 0–100 A.

The potential drop across the specimen was measured using a Lindek circuit. Potential differences of $10^{-8}\mu\text{V}$ could be readily detected, and an emf of $1\mu\text{V}$ could be measured to 1%. This accuracy increased with the emf until it reached 0.04%, which was the precision of the standard resistors used in the Lindek circuit.

In order to eliminate the effect of thermal emf's in the circuit, the potential across the specimen was measured for a particular value of the current in both directions, and the two values of the resistances were averaged. In actual practice thermal emfs never exceeded $0.5\mu\text{V}$.

Cryostat and the Measurements of Temperature

The specimen, together with the plate on which it was mounted, was suspended by means of a thin walled stainless steel tube in a glass helium Dewar surrounded by liquid nitrogen. The cryostat was pumped through a Walker²¹ pressure regulator by means of an oil rotary pump with a displacement of 300 cu ft per minute. For temperatures down to the lambda point, the bath was stirred by a 36-mW heater at the bottom of the cryostat.

²⁰ R. W. Powell, Proc. Roy. Soc. (London) **A209**, 525 (1951).

²¹ E. J. Walker, Rev. Sci. Instr. **30**, 834 (1959).

The vapor pressure of He was measured by means of a mercury manometer down to 10 mm of Hg, and below this pressure by an oil manometer. The pressures were then converted into temperatures using the T_{58} scale. Above the lambda point, corrections were applied for the hydrostatic pressure of liquid helium measured from the center of the specimen. It was estimated that the uncertainty in the values of temperatures quoted for small currents through the specimen are approximately $\pm 0.005^\circ\text{K}$. The lowest temperature which could be attained in this cryostat was 1.2°K . This high value was due to a large heat influx caused by conduction along the two pairs of No. 22 copper wires used to lead the current of the specimen. These were necessary in order to investigate the dependence of the resistance on the measuring current. Currents up to 50 A could be passed through these wires without altering the temperature more than 0.01°K . During the course of measurements, it was found that the field generated by the current through the specimen strongly influenced the value of its resistance. To study this effect in detail it became necessary to keep the return current leads as far away from the specimen as possible. In practice, the field at the surface of the specimen due to the return current was never allowed to exceed 3% of the field due to the current through the specimen itself.

Magnetic Fields

The effect of a longitudinal magnetic field on the resistance of these specimens was studied by means of a superconducting solenoid surrounding the specimen in the helium bath. The solenoid was wound on a Bakelite cylinder 10 in. long and 3 in. in diameter with 7200 turns of unannealed niobium wire of 0.004 in. diam. It was capable of producing a maximum field of 1380 G, which was uniform to one percent over an axial length of 2.8 in.

TABLE I. Thermal expansion data used to calculate specimen dimensions at various temperatures, $a = \Delta L / L \Delta t$ is the linear expansion coefficient per degree centigrade L_{24} is the length at 24°C.

Crystal orientation	Temperature between 0 and 30°C per degree centigrade	Length correction ΔL for a temperature change from 24°C to 77°K	Length correction ΔL for a temperature change from 24°C to 2.4°K
A axis	$a_A = 1.15 \times 10^{-5}$	$(\Delta L / L_{24})_A = -2.16 \times 10^{-3}$	$(\Delta L / L_{24})_A = -2.41 \times 10^{-3}$
B axis	$a_B = 3.15 \times 10^{-5}$	$(\Delta L / L_{24})_B = -6.06 \times 10^{-3}$	$(\Delta L / L_{24})_B = -6.99 \times 10^{-3}$
C axis	$a_C = 1.65 \times 10^{-5}$	$(\Delta L / L_{24})_C = -3.16 \times 10^{-3}$	$(\Delta L / L_{24})_C = -4.11 \times 10^{-3}$

A transverse field was applied to the specimens by means of a pair of Helmholtz coils designed according to a method described by Garrett.²² Each coil was 10 in. in radius and the pair produced a field of 17.4 G/A up to a maximum of 500 G. These coils formed a fourth-order system in Garrett's notation, with a uniformity of 1% over a spherical volume of 6 in. diam.

III. RESULTS

The Mean Free Path of Electrons and the Temperature Dependence of Resistivity

The resistance of the crystals was found to be strongly dependent on the measuring current. This effect and its implications will be discussed in detail in a later section.

In this section the resistances are the limiting resistances defined by

$$R_0 = \lim_{I \rightarrow 0} (V/I), \tag{3.1}$$

where V is the potential and I the current.

R_0 was determined for each specimen at seven different temperatures between 4.2° and 1.2°K and fitted to the expression

$$R_0(T) = R_r + \alpha T^n. \tag{3.2}$$

Since it was difficult to obtain an accurate value of the residual resistance R_r directly from the observations, the following procedure was adopted. An approximate value for R_r was first obtained by plotting R_0 as a function of temperature and extrapolating the curve to $T = 0^\circ\text{K}$. We then plotted a graph of $\log_{10}[R(T) - R_r]$ against $\log_{10} T$ for a number of values of R_r close to the extrapolated value and on either side of it, and finally selected the value of R_r which made this graph most nearly a straight line. This is illustrated in Fig. 3 which represents the observations for crystal C_6^1 . In this way we not only obtained the best value of R_r , but also were able to set a limit to the uncertainties involved. In Table II, we tabulate the results of our measurements for the six C-axis crystals. All the values of resistivity at 0°C and 77°K in this table agree with one another and indicate that the crystals were free of defects. Our values for these two temperatures agree with

those of Powell²⁰ and Olsen-Bar and Powell²³ who obtained resistivities of 51.3×10^{-6} and $10.5 \times 10^{-6} \Omega\text{-cm}$ for 0°C and 77°K, respectively.

For a given temperature the resistances were fitted to Eq. (1.3) by the method of least squares. The calculated slopes and the bulk resistivities given by the intercepts at $1/d = 0$ are listed in Table III. These results are also displayed in Fig. 4 for $T = 4.2^\circ$ and 0°K , along with the most probable straight lines. The much larger scatter in ρ_r than in $\rho_{4.2}$ is presumably due to the fact that at lower temperatures the variation of the resistance as a function of the measuring current becomes much more pronounced and therefore it is more difficult to obtain reliable values by extrapolating the resistance to zero measuring current. The calculated values of the slope and the bulk residual resistivity for the lower straight line in Fig. 5 are $7.27 \times 10^{-11} \Omega\text{-cm}^2$ and $-3 \times 10^{-11} \Omega\text{-cm}$, respectively. Since a negative value for resistivity is impossible, it is safe to assume that within the accuracy of our measurements it is zero and this shows that at $T = 0^\circ\text{K}$ $d/l_b \ll 1$ for all the crystals. From Eq. (1.8), we know that for wires of square cross section,

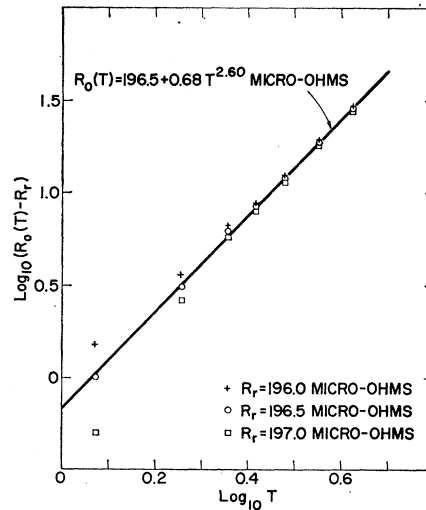


FIG. 3. Temperature dependence of the resistance of the C_6^1 specimen.

²² M. W. Garrett, J. Appl. Phys. 22, 1091 (1951).

²³ M. Olsen-Bar and R. W. Powell, Proc. Roy. Soc. (London) A209, 542 (1951).

TABLE II. Characteristics of the crystals used in this work. The crystals have a square cross section with d as the side of the square. The specimens are labeled with a C to designate the direction of current flow relative to the crystalline axes; the subscript is the specimen number; the superscript indicates that batch of gallium from which the specimen was grown. For temperatures between 1.2 and 4.2°K, the resistivities of these specimens were fitted to an expression of the form $\rho(T) = \rho_r + \alpha T^n$ Ω -cm.

Specimen	symbol	Length between probes at 0°K (cm)	d at 0°K (cm)	$1/d$ at 0°K (cm ⁻¹)	ρ at 0°K (10 ⁻⁶ Ω -cm) ^a	ρ at 77°K (10 ⁻⁶ Ω -cm)	ρ at 4.2°K (10 ⁻¹⁰ Ω -cm)	ρ_r at 0°K (10 ⁻¹⁰ Ω -cm)	$\alpha \times 10^{11}$	n
C ₁ ²	○	7.55	0.102	9.82	51.9	10.46	12.7	6.45 ± 0.15	4.7 ± 0.7	1.81 ± 0.1
C ₂ ²	△	6.83	0.0513	19.50	...	10.46	20.9	15.3 ± 0.12	0.50 ± 0.12	3.28 ± 0.16
C ₃ ¹	□	6.84	0.0373	26.80	52.0	10.64	26.5	18.9 ± 0.10	2.84 ± 0.6	2.29 ± 0.1
C ₄ ¹	△	4.80	0.0206 ^b	48.54	51.3	10.46 ^b	43.1	34.7 ± 0.1	2.21 ± 0.4	2.51 ± 0.1
C ₅ ²	+	4.48	0.0171	58.63	53.6	10.60	51.4	40.9 ± 0.7	4.15 ± 0.4	2.24 ± 0.1
C ₆ ¹	◇	4.06	0.0115	87.00	52.2	10.55	73.1	63.9 ± 0.1	2.21 ± 0.03	2.60 ± 0.1

^a The specimens were not in good thermal contact with the ice bath; consequently these resistivities correspond to temperatures ranging from 1 to 5°K.

^b This specimen was accidentally destroyed before its dimensions could be measured; d was therefore deduced from its resistance at 77°K using a value of 10.46×10^{-6} Ω -cm for the resistivity.

the slope is $\rho_b l_b / 1.116$ for free electrons. Therefore, we have

$$(\rho_b l_b)_C = 8.11 \times 10^{-11} \Omega\text{-cm}^2$$

for current flowing along the C axis.

If we substitute the appropriate values of the Fermi momentum and the number of electrons per unit volume for gallium in 1.2 (see Appendix B), we obtain

$$\rho_b l_b = 4.42 \times 10^{-12} \Omega\text{-cm}^2.$$

This indicates that, for conduction along the C axis, gallium contributes only 0.04 electrons per atom instead of all the 3 available outside the closed $3d$ shell.

Although the accuracy of our measurements does not allow us to determine a precise value for the bulk resistivity at $T = 0^\circ\text{K}$, we can set an upper limit of 8×10^{-11} Ω -cm from the scatter of points in Fig. 4. This means that the mean free path of electrons in the bulk metal ≥ 1 cm. Roberts,²⁴ from measurements of ultrasonic resonance in gallium, also concludes that the mean free path of electrons at 1.5°K is of the order of 1 cm.

From column 3, Table III, we find that the slope A steadily increases with temperature. In order to test the validity of Olsen's¹² explanation for this increase, we compare our results with Eq. (1.9) derived by Blatt

and Satz, which can be rewritten as

$$\rho_d(T) = \rho_b(T) + [(0.727/d) + \epsilon(0.811/d)^{2/3}] \times 10^{-10} \Omega\text{-cm}, \quad (3.3)$$

where the appropriate values of $\rho_b l_b$ and the slope A have been substituted from our observations. Here

$$\epsilon = [8\pi f \rho_i(T)]^{1/3} (T/\Theta_D)^{2/3} \times 10^{10/3}. \quad (3.4)$$

From Eq. (3.3), it is clear that a plot of $[10^{10} \rho_d(T) - (0.727/d)]$ against $(0.811/d)^{2/3}$ should give a straight line whose slope is ϵ and whose intercept at $1/d = 0$ gives the bulk resistivity. Figure 5 shows the results of this calculation for different temperatures. The straight lines in this figure have been drawn by calculating their slopes by the method of least squares. The agreement, which is extremely good at 4.22°K, gets steadily worse as the temperature is lowered. This may be partly due to the fact that the lower the temperature the lower is the accuracy with which we could obtain $\lim_{I \rightarrow 0} (V/I)$.

The bulk resistivities and the slopes obtained from these calculations are tabulated in columns 4 and 5 of Table III. Here $\rho_b(T)$, the bulk resistivity at a given temperature, is the sum of two terms and can be written

TABLE III. Calculated slopes and the bulk resistivity given by the intercepts at $1/d = 0$.

T (°K)	ρ_d versus $1/d$		$\left(10^{10} \rho_d - \frac{0.727}{d}\right)$ versus $(0.811/d)^{2/3}$		Calculated by using $\rho_b(T) = 2.5T^{4.5} \times 10^{-13}$ Ω -cm	
	Intercept at $1/d = 0$ (10 ⁻¹⁰ Ω -cm)	Slope A (10 ⁻¹⁰ Ω -cm ²)	Intercept at $1/d = 0$ ρ_b (10 ⁻¹⁰ Ω -cm)	Slope ϵ	Slope ϵ_{calc}	
4.22	5.17	0.787	4.44	0.33	0.20	
3.56	3.47	0.762	2.84	0.21	0.14	
3.02	2.46	0.754	2.02	0.12	0.10	
2.60	1.76	0.738	1.38	0.09	0.076	
2.26	1.28	0.733	0.95	0.06	0.052	
1.80	0.81	0.726	0.62	0.02	0.032	
1.20	0.30	0.720	0.28	-0.02	0.016	
0	-0.32	0.727	0.000	

²⁴ B. W. Roberts, Phys. Rev. Letters 6, 453 (1961).

as

$$\rho_b(T) = \rho_i(T) + \rho_r, \quad (3.5)$$

where $\rho_i(T)$ is the ideal resistivity which is temperature-dependent, and ρ_r is the residual resistivity due to impurities and lattice defects.

Although there is no direct way of separating these two terms from the above data, we can utilize the fact that the ideal resistivity, for a limited region of temperature, is expected to follow a power law in temperature, which means that a plot of $\log[\rho_b(T) - \rho_r]$, with a correct value of ρ_r , against $\log T$ should give a straight line. In Fig. 6, therefore, we have plotted these two quantities for the two arbitrarily chosen values 0 and $5 \times 10^{-11} \Omega\text{-cm}$ for ρ_r . Since it is impossible to imagine a process which would enhance the temperature dependence of the ideal resistivity as the temperature falls, it is clear that within the precision of our measurements the residual resistivity is zero. A conservative upper limit of $2 \times 10^{-11} \Omega\text{-cm}$ would imply a mean free path of 4 cm as a lower limit for scattering by impurities or

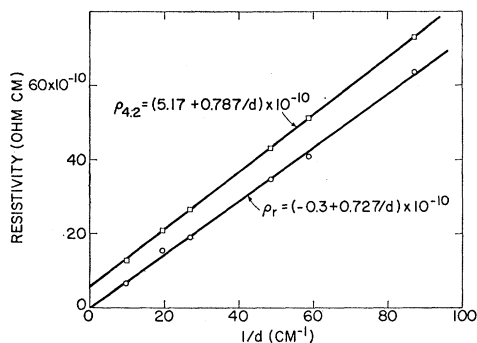


FIG. 4. Resistivity of *C*-axis wires as a function of the reciprocal of the specimen dimension d at a constant temperature. \square —4.2°K \circ —0°K.

lattice defects. Figure 6 also shows that the ideal resistivity of gallium varies at $T^{2.4}$ between 2.26° and 4.2°K.

Theory predicts that for normal electron-phonon collisions the ideal resistivity should be proportional to T^5 at low temperatures, and this is very nearly true for most pure metals. For gallium, both Olsen-Bar and Powell²³ and Weisberg and Josephs²⁵ have established a variation proportional to $T^{4.5}$ for a temperature range of 5 to 20°K. Peierls²⁶ originally pointed out that in a pure metal the resistivity, at sufficiently low temperatures, should be governed by electron-electron collisions and a T^2 variation should describe the ultimate behavior of the ideal resistivity. Pines²⁷ has pointed out that the conditions for observing this contribution would be most favorable in a metal which has an impurity

²⁵ L. R. Weisberg and R. M. Josephs, *Phys. Rev.* **124**, 36 (1961).

²⁶ R. E. Peierls, *Quantum Theory of Solids* (Oxford University Press, London, 1955).

²⁷ D. Pines, *Elementary Excitations in Solids* (W. A. Benjamin Inc., New York, 1963).

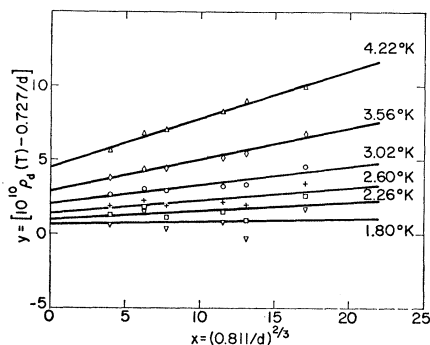


FIG. 5. A comparison of our results with Eq. (3.3).

concentration of the order of 10^{-8} and is strongly anisotropic. Both these conditions are well satisfied in these gallium crystals and therefore it is reasonable to assume that the $T^{2.4}$ temperature dependence is due to electron-electron scattering becoming more dominant than the normal electron-phonon collisions. It is interesting to note that the last three points at the low temperature end of Fig. 6 lie on a straight line which follows an exact T^2 dependence. This, however, is of no great significance because it is in precisely this region that the disagreement between theory and experiment is most marked and the extrapolated values of ρ_b are likely to be in error. Clearly the question cannot be finally settled unless this region is investigated in greater detail, with much greater precision and larger specimens. We have also calculated the temperature dependence of the ideal resistivity from the intercepts of the direct ρ_d versus $1/d$ straight lines (column 2, Table III) and find that it varies as $T^{2.25}$. Although it is realized that this value, which neglects the temperature increase of the slope, is likely to be even less accurate than the preceding value, the main conclusion which seems inevitable, and which must be emphasized, is that the ideal resistivity is varying very nearly as predicted by electron-electron

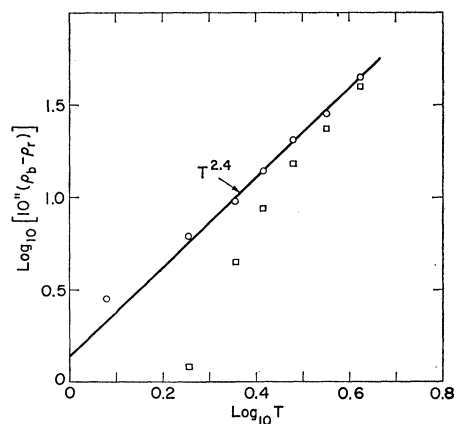


FIG. 6. The temperature dependence of the bulk resistivity ρ_b . The circles assume the residual resistivity to be zero and the squares assume it to be $5 \times 10^{-11} \Omega\text{-cm}$.

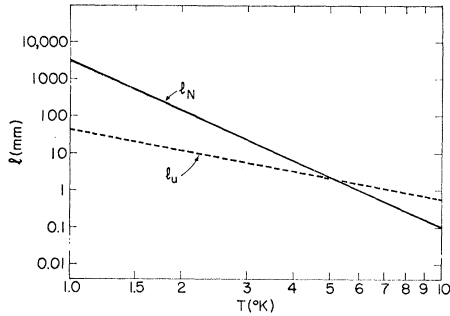


FIG. 7. The bulk mean free path of electrons as a function of temperature. l_N represents normal electron-phonon collisions and l_u represents collisions which may be umklapp or electron-electron.

interaction. However, in this temperature region, the possibility of contributions due to electron-phonon umklapp processes cannot be completely neglected. In all probability the temperature dependence in the entire region is due to the combined efforts of electron-electron and electron-phonon umklapp and normal processes.

According to the above interpretation, the normal electron-phonon collisions would dominate the resistance in the temperature range in which Olsen-Bar and Powell²³ and Weisberg and Josephs²⁵ have shown a $T^{4.5}$ variation, whereas at lower temperatures the electron-electron events would become more important. Neither Olsen-Bar and Powell nor Weisberg and Josephs could have observed this because their gallium was much less pure and its resistance had already approached a constant value at 4.2°K. Let us suppose that the $T^{2.4}$ variation is due to a combined action of the normal and, for lack of a better term, abnormal processes. The ideal resistivity can then be written as

$$\rho_i(T) = \beta T^m + \gamma T^{4.5} \quad (3.6)$$

on the assumption that $T^{4.5}$ is a true representation of the normal electron-phonon contribution. Substituting the values of $\rho_i(T)$ from our observations we can determine numerical values of β , γ , and m . As a result of this calculation, Eq. (3.6) becomes

$$\rho_i(T) = (2.5T^{4.5} + 190T^{1.9}) \times 10^{-13} \Omega\text{-cm.} \quad (3.7)$$

Once again, $T^{1.9}$ is so close to T^2 that it is difficult not to attribute this to an electron-electron resistance. There is no general rule for determining the temperature variation of electron-phonon umklapp processes, and it is possible that their contribution by coincidence also follows a T^2 variation. However, these processes by their very nature should depend on the geometry of the Fermi surface and therefore it is possible that in gallium, whose Fermi surface is very anisotropic, their contribution along different axes would be different. Our observations for the other two axes, details of which are to be published in another paper, also show a variation very

close to T^2 and the conclusion that this is a consequence of electron-electron collisions seems unavoidable.

From Eq. (3.7) and the experimental value of $(\rho_b l_b)_c$ obtained above, we have calculated separately the mean free paths for the two mechanisms as a function of temperature. The result is illustrated in Fig. 7 which clearly shows that below 4°K, the resistance is no longer governed by normal electron-phonon collisions and for this reason electron-electron or umklapp processes can become effective. At higher temperatures, normal processes begin to take over and achieve complete dominance at about 10°K. It is now clear why a mean free path of the order of 1 mm due to impurities makes it impossible for the temperature to change the resistance of gallium below 4°K.

Finally, we can compare the values of the slope ϵ (columns 5 and 6, Table III) obtained directly from the size effect observations with those obtained by substituting the first term on the right-hand side of Eq. (3.7) in Eq. (3.4) with $f=1$, and using Seidel and Keesom's²⁸ value of 300°K for the low-temperature Debye Θ of gallium. The temperature variation of this slope is proportional to $T^{2.17}$ for the calculated values and to $T^{2.9}$ for the observed (see Fig. 8). This discrepancy, which also exists for In and Hg,¹⁴ stresses the fact that the Blatt and Satz calculations are very approximate.

Longitudinal Magnetoresistance

Working with thin sodium wires, MacDonald²⁹ in 1949 was the first to discover that the resistivity, instead of increasing as for the bulk metal, actually decreases with the application of a longitudinal magnetic field. This was attributed by him to the lengthening of the effective mean free path caused by the spiral motion of the electrons around the lines of the magnetic field. Chambers⁷ has developed an exact analysis of this effect based on the free electron model assuming diffuse scat-

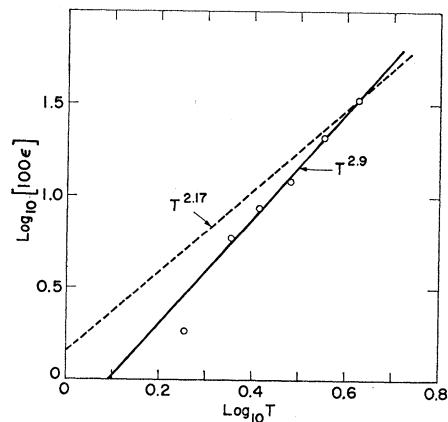


FIG. 8. Temperature dependence of the coefficient ϵ of Eq. (3.4).

²⁸ G. Seidel and P. H. Keesom, Phys. Rev. **112**, 1083 (1958).

²⁹ D. K. C. MacDonald, Nature **163**, 637 (1949).

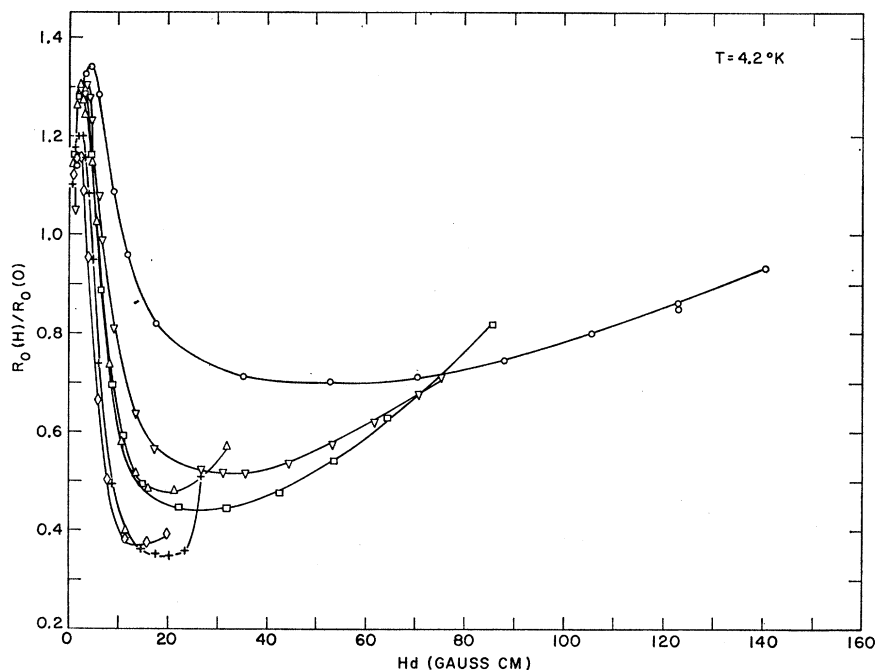


FIG. 9. Normalized resistance as a function of the longitudinal field times the dimensions of the crystals. Symbols are identified in Table II.

tering at the boundaries. The final results derived by Chambers depend on two parameters, d/r_0 where r_0 is the cyclotron radius, and d/l_b the ratio of the dimensions of the wire to the mean free path. For a fixed value of d/l_b provided $d/l_b < 1$ the resistance begins to decrease with increasing field until it reaches the bulk value as d/r_0 tends to infinity. The smaller the ratio of d/l_b , the more rapid is the initial rate of decrease of resistance as a function of d/r_0 . It must be pointed out that Chambers' theory is based on the free-electron model and neglects the phenomenon of bulk magnetoresistance shown by all metals in varying degrees.

Since MacDonald's initial discovery, the effect has also been observed in Sb³⁰, Bi³¹, In^{12,32,33}, Sn, Zn, Al, Cd, and Pb³⁴ more or less in accordance with Chambers' predictions.

We have also investigated the effect of a longitudinal field on the resistivity of our crystals at 4.2° and 1.2°K up to a maximum of 1400 G. The field was parallel to the axis of the crystals to within 2 or 3°. In order to compare our results with those of Chambers we have plotted our measurements in Figs. 9 and 10 showing $R_0(H)/R_0$, where R_0 is the limiting resistance of Eq. (3.1) and $R_0(H)$ the same in a field H , as a function of the product of the magnetic field strength and the size

of the wire. Since $H \propto 1/r_0$, our way of presenting the results is equivalent to that of Chambers. As expected, the resistance does indeed drop rapidly as a function of the field, but instead of approaching a limiting value it begins to rise after going through a minimum. Initially, it also shows a maximum which can be seen more clearly in Figs. 11 and 12, where the low-field values have been replotted on an enlarged scale. Both these features, which are not predicted by the free electron theory, are exhibited by all the above metals except Na and can be attributed to the presence of bulk magnetoresistance. As soon as the field is applied, the charge carriers begin to spiral round and the resistance tends to decrease; at the same time the bulk magnetoresistance also begins to play its part. Therefore, the net change in resistance which we observe is due to the combined effects of the two phenomena taking place simultaneously. In other words, $\rho_d(H)/\rho_d$, which we plotted in Fig. 9, is in reality the product of $\rho_d(H)/\rho_d$, which Ga would show if somehow we could suppress its bulk magnetoresistance, and $\rho_B(H)/\rho_B$ which is the ordinary bulk magnetoresistance.

In order to show that these two phenomena acting simultaneously do indeed give results similar to those of Fig. 11, we have plotted in Fig. 13 the quantity

$$\rho_d(H)/\rho_d = [\rho_d(H)/\rho_b(H)][\rho_b/\rho_d][\rho_b(H)/\rho_b] \quad (3.8)$$

for Ga, assuming different values of d and d/l_b . It was assumed that the first factor in Eq. (3.8) is given by Chambers' free-electron theory using the value r_0 from Appendix B, the second factor was set equal to $1.116 d/l_b$ [Eq. (1.8)], and the last factor was obtained by extrapolating to zero magnetic field the actual bulk

³⁰ M. C. Steele, Phys. Rev. **97**, 1720 (1955).

³¹ J. Babitskin, Phys. Rev. **107**, 981 (1957).

³² P. Cotti, Helv. Phys. Acta **33**, 517 (1960).

³³ C. Froidevaux, J. R. Keyston, P. Cotti, and J. L. Olsen, in *Proceedings VII International Conference on Low Temperature Physics, Toronto, 1960* (University of Toronto Press, Toronto, 1960).

³⁴ B. N. Alexandrov, Zh. Eksperim. i Teor. Fiz. **43**, 1231 (1962) [English transl.: Soviet Phys.—JETP **16**, 871 (1963)].

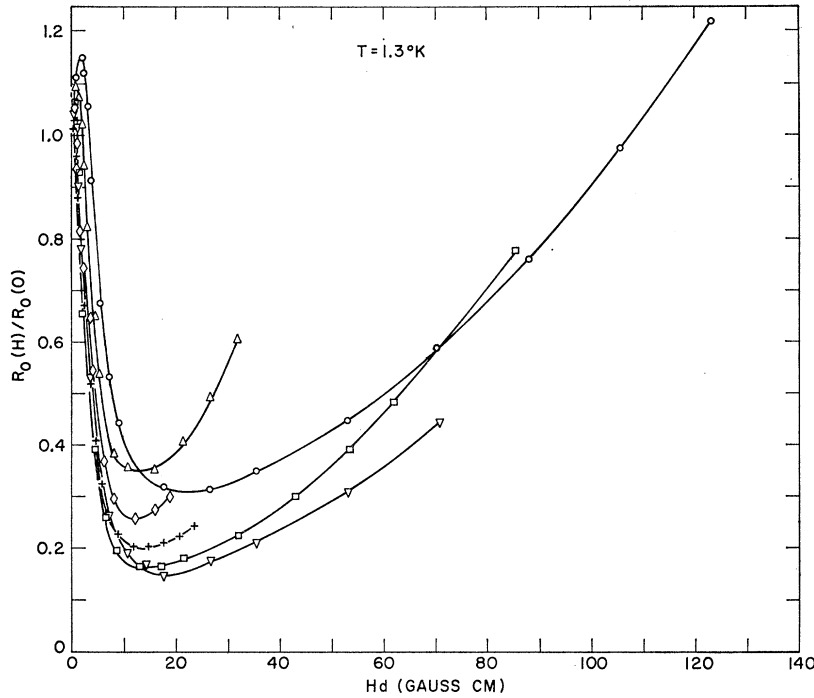


FIG. 10. Normalized resistance as a function of the longitudinal field times the dimensions of the crystals. Symbols are identified in Table II.

magnetoresistance shown by our crystals at higher values of the longitudinal field. In spite of the fact that Chambers' theory is not strictly valid for complicated metals such as gallium, Fig. 13 does indeed display all the features observed in the experimental curves. The maximum appears in the beginning because initially the bulk magnetoresistance rises more rapidly than the fall due to boundary effects. However, the rate of change of the bulk resistance with field is independent of size, whereas the rate of decrease of resistance with the field becomes more rapid as the ratio d/l_b becomes smaller. The result is that for smaller specimens the maximum is less marked and appears at a lower value of the field. For the purpose of direct comparison with the calculated curves, we have also plotted in Fig. 13 the experi-

mental points at 1.2°K for the C_1^3 crystal whose dimensions are the same as those for the middle curve and whose ratio of d/l_b from the simple size-effect measurements is known to be $\approx 1/100$. The much more rapid drop in its resistance compared with the middle curve indicates that the average momentum of the electrons for a plane perpendicular to the C axis is about half the free-electron value. This has been estimated from the low-field region in which the experimental points and the middle curve in Fig. 13 differ by a factor of about 2 in the value of the field for the same relative drop in resistance. The agreement between the points and the curve improves as we go to higher fields but this has no particular significance because the latter part of the calculated curve has been obtained by using the actual

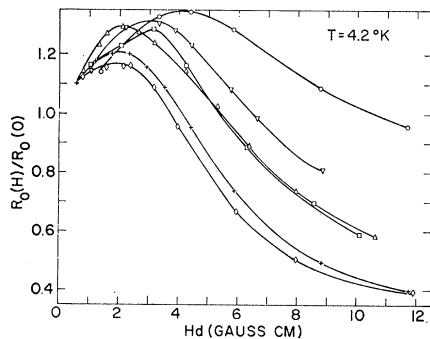


FIG. 11. Normalized resistance as a function of the longitudinal field times the dimensions of the crystals for low values of the field showing an initial increase in the resistance for every crystal.

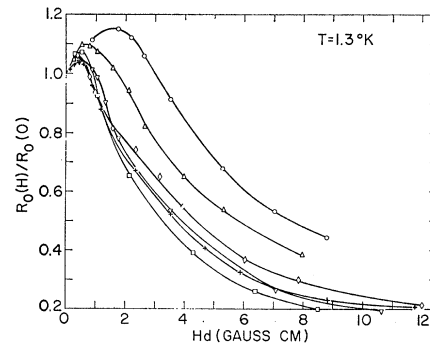


FIG. 12. Normalized resistance as a function of the longitudinal field times the dimensions of the crystals for low values of the field showing an initial increase in the resistance for every crystal.

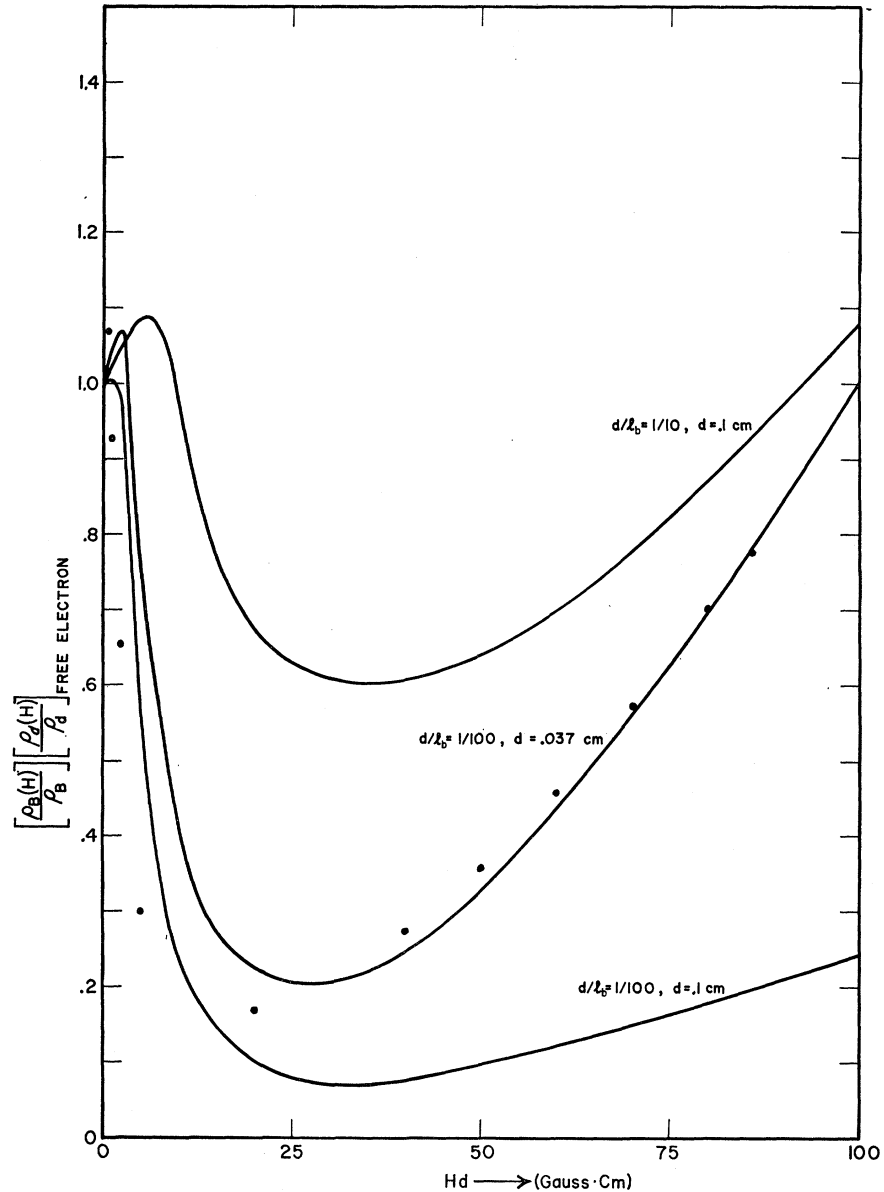


FIG. 13. The product of the longitudinal magnetoresistance for free electrons and the bulk longitudinal magnetoresistance as a function of Hd for different ratios of d/l_b .

experimental values of the bulk magnetoresistance shown by the specimens themselves.

Transverse Magnetoresistance

MacDonald²⁹ in 1949 discovered that the resistance of thin Na wires falls not only in a longitudinal but also in a transverse field. This result was unexpected since it is difficult to visualize from simple physical arguments how a transverse field can affect the conductivity at all. The presence of a nonuniform Hall field, whose magnitude and direction have to be taken into account, makes it almost impossible to formulate an exact theory for the effect of a transverse field on thin wires. MacDonald and Sarginson⁸ have worked out an approximate solution of the influence of a transverse field on a thin film whose

plane is parallel to the field. Assuming diffuse scattering at the walls, they show that the resistance of the film decreases as a function of the field. They then go on to show a qualitative agreement between their calculations and experimental results on Na wires. The reduction of the resistance, however, is so small that the effect would be completely obliterated by the presence of any bulk magnetoresistance. Nevertheless, the existence of appreciable magnetomorphic effects can be expected to alter the field dependence shown by the bulk metal. It is well known^{36,37} that in a transverse field, the magneto-

²⁹ A. J. Bradley, Z. Krist. **91**, 302 (1935).

³⁶ J. H. Condon, Bull. Am. Phys. Soc. **9**, 239 (1964).

³⁷ A. Goldstein and S. Foner, Bull. Am. Phys. Soc. **9**, 239 (1964).

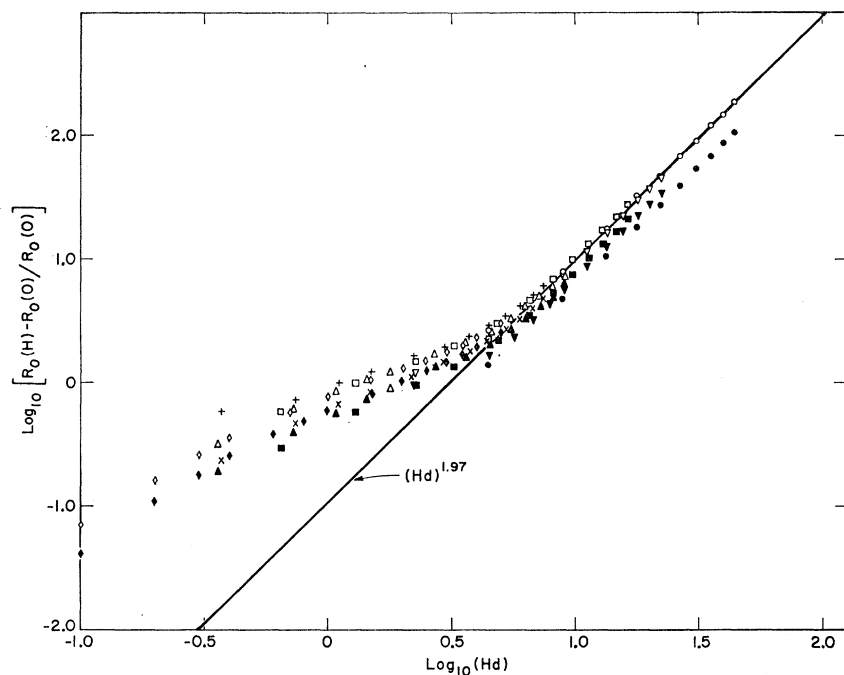


FIG. 14. The magnetic field dependence of the transverse magneto-resistance. The symbols are identified in Table II. Open symbols are for 1.3°K and black for 4.2°K.

morphic effects eventually disappear when the cyclotron radius of the charge carriers become much less than the dimensions of the specimen. At and beyond this stage the magneto-resistance would be expected to regain its bulk field dependence. Such behavior is indeed displayed by most of our specimens in a transverse field as can be seen in Fig. 14, which is a plot of $\log_{10}(\Delta R/R)$ against $\log_{10} Hd$. A transverse field up to a maximum of 400 G was applied to each specimen and was parallel to the A axis to within about 2 deg. Measurements were made both at 4.2° and 1.2°K. At low values of the field, each specimen seems to follow a different curve. However, at a value of approximately 5 for Hd , all curves, after changing from concave down to concave up, bend sharply upwards. Beyond this point they appear to be parallel to each other and we conclude that in this region they represent the bulk magneto-resistance only. The appearance of the bend for the same value of Hd , which is proportional to d/r_0 , is a clear indication of the fact that the bulk behavior is reached when the cyclotron radius of the charge carriers attains a fixed ratio with respect to the dimensions of the specimen. According to Kohler's rule, the magneto-resistivity function, $\Delta R/R$, depends upon magnetic field and mean free path through the product (Hl_b) . The data for all of the specimens at 1.2°K fall very nearly on the same curve, from which it can be concluded that the specimen walls are playing the role of a mean free path even for the specimen 1 mm on a side (the motion of the carriers parallel to the magnetic field is unaffected by the field). This is additional evidence that the mean free path in these gallium crystals at 1.2°K is very long.

If $d/r_0 \gg 1$ at $Hd=5$, then it is clear that on an average the orbit of electrons in a plane perpendicular to the A axis has a momentum which is at least 10 times smaller than the momentum of the free electrons at the Brillouin zone. In view of the complexity of the gallium energy bands (see Slater, Koster and Wood³⁸ and Reed and Marcus³⁹) this result is not too unexpected. It is also consistent with the results of de Haas-van Alphen effect on Ga reported by Shoenberg,⁴⁰ Condon,³⁶ and Goldstein,³⁷ who show that for different directions of the magnetic field, the momentum ranges from one half to one thousandth of its value at the Brillouin zone. If we extrapolate our results for the 1-mm crystal at 4.2°K to a field of 12 kG, we get $\Delta R/R_0 = 6 \times 10^4$. For a 1-mm crystal under identical conditions, Reed and Marcus³⁹ obtained a value of 4×10^4 . Considering that their Ga was not as pure as ours, the two values are in reasonable agreement.

Current Dependence of the Resistance

The resistance of our crystals, defined as $R=V/I$, where V is the potential and I the current through the specimen, was found to depend in a complicated way on the current. This can be seen for all six crystals in Fig. 15.

It is clear that such complex variations could not be entirely due to the Joule heating of the crystals by the current. However, it was necessary to make sure that

³⁸ J. C. Slater, G. F. Koster, and J. Wood, Phys. Rev. **126**, 1307 (1962).

³⁹ W. A. Reed and J. A. Marcus, Phys. Rev. **126**, 1298 (1962).

⁴⁰ D. Shoenberg, Phil. Trans. Roy. Soc. (London), **245**, 1 (1952).

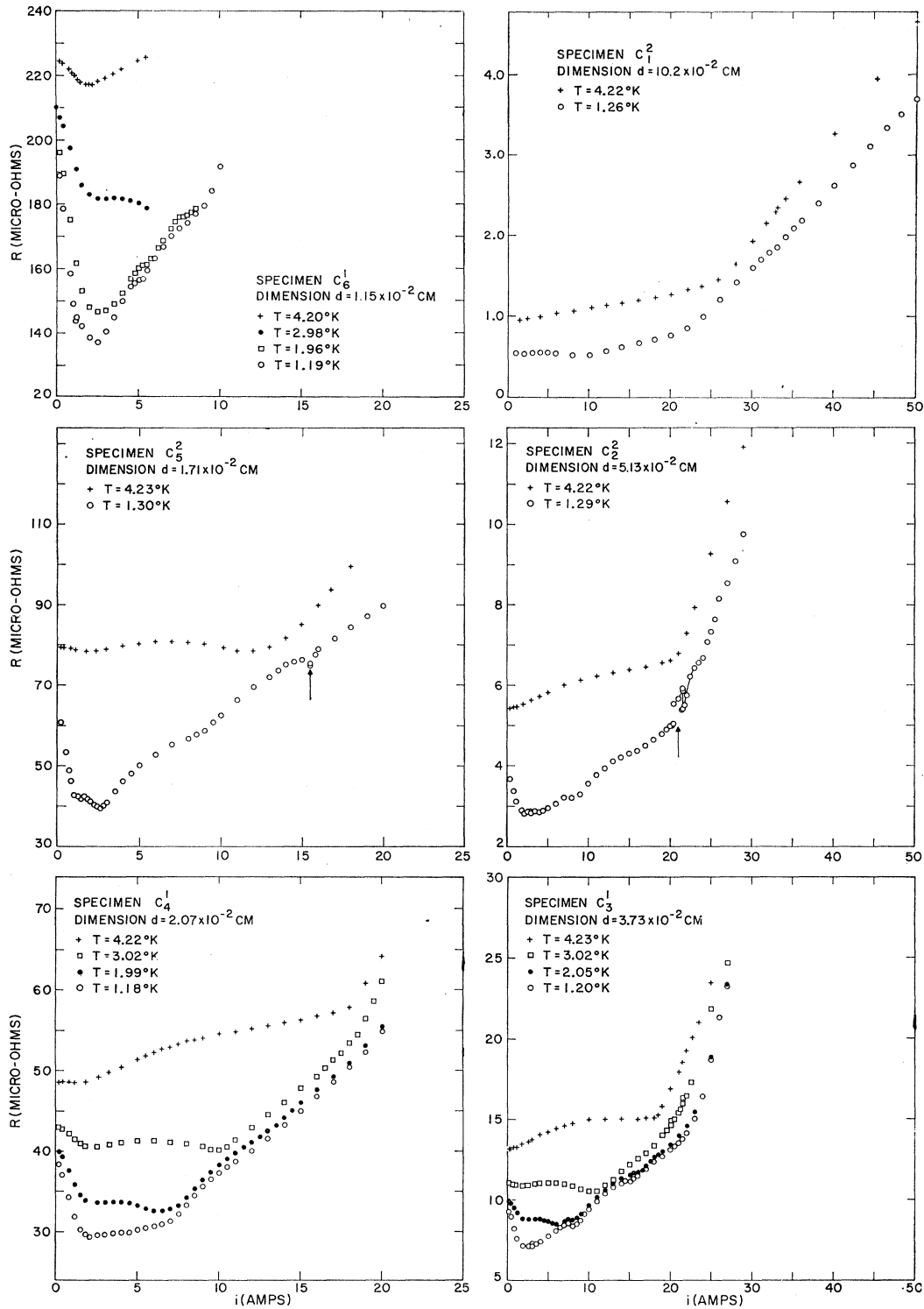


FIG. 15. The current dependence of the resistance for the C-axis crystals of different size.

heating contributed nothing to the observed phenomena. The current regulator was designed to keep the value of the current through the crystal at a pre-selected value,

irrespective of any changes in the resistance of the circuit. If, at a certain stage, the dissipation of Joule heat became large enough to cause a rise of temperature in

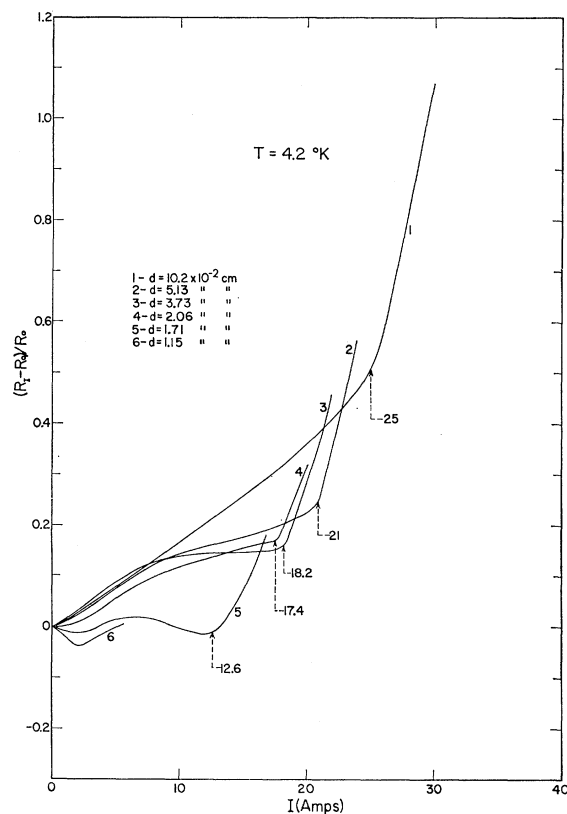


FIG. 16. $\Delta R/R_0$ as a function of the current for the six crystals at 4.2°K.

the specimen, its resistance also increased as a consequence. With a constant current, the dissipation of heat continued to increase so rapidly that within a fraction of a second, the crystal reached its melting point and was destroyed. At the cost of destroying several crystals in this way, we arrived at a value of 0.4 W/cm² at 4.2°K for the critical power density below which the temperature of the crystal did not rise above that of the bath. In actual measurements, therefore, we never exceeded 0.21 W per cm². Here, it might be of interest to mention that our critical value agrees with the observations of Eastman and Datars,⁴¹ who found that the resistance of single crystals of Sb, Bi, As, and Te displayed an anomalous increase at 4.2°K if the power input exceeded 0.5 W/cm².

In a preliminary account of this phenomenon, the dependence of the resistance on the measuring current was attributed to the magnetoresistive effects of the field generated by the measuring current itself. The bulk magnetoresistance is always positive in all metals and for small fields always increases as a function of the field. It is therefore clear that the initial fall in the resistance, which is characteristic of all specimens at 1.2°K, could not be caused by the phenomenon of bulk magnetoresistance. However, it is well known that in speci-

mens of small size, the effect of the boundary scattering can be altered considerably by the bending of electrons round the magnetic field. This, in general, leads to a nonzero change in resistance which may be positive or negative. The details of the phenomenon strongly depend on the shape of the specimen and the relative configuration of the current and the magnetic field. They are purely classical in nature, and entirely different from the bulk effects. We believe that a joint action of these so-called galvanomagnetomorphic effects and bulk magnetoresistance is responsible for the complex nature of the curves in Fig. 15.

The field due to the current is essentially a transverse field which has the property of deflecting the electrons, moving opposite to the direction of the current, away from the walls. Thus, the mean free path, which in the absence of a field will be limited by scattering at the walls, is lengthened and causes the resistance to decrease.

In Fig. 16, we have plotted $\Delta R/R_0$ for all six specimens at 4.2°K. The characteristics of the curves in this figure can be summarized as follows:

- (1) Towards the end, each curve has a sharp upward bend which becomes more pronounced as the specimen size is decreased.
- (2) The smaller the specimen the lower is the value of the current at which the bend appears.
- (3) The smaller the dimensions, the lower is the value of $\Delta R/R_0$ at the bend.
- (4) The slope for small values of the current, which is positive in the larger specimens, decreases as the dimensions become smaller; for the two smallest specimens, the initial slope is negative and a distinct minimum appears at about 2.5 A.

At a fixed temperature, reducing the size of the specimen reduces the ratio d/l_b . In a single specimen, this ratio can be reduced by lowering the temperature. If the change in the characteristics of the curves described above is a consequence of the reduction in d/l_b only, then in one and the same specimen, we should expect a curve for a lower temperature to be similar in shape to a curve for a smaller specimen at a higher temperature. That this indeed is the case can be seen in Fig. 17, which displays $\Delta R/R_0$ against I for the C_3^1 specimen at different temperatures; curve 2 of this figure is remarkably similar to curve 5 of Fig. 16. Since the lowering of the temperature reduces the ratio d/l_b much more drastically, we find that in curve 3, which is for 2°K, the initial negative slope is steeper and the sharp bend appears at a still lower value of the current. Further lowering of the temperature makes the initial drop even more rapid and two additional minima make an appearance.

The Fermi surface of gallium is very complicated. According to Reed and Marcus,³⁹ it is composed of seven bands. There are three hole bands and three elec-

⁴¹ P. C. Eastman and W. R. Datars, *Cryogenics* 3, 40 (1963).

tron bands and one band which has both holes and electrons. The number of holes and electrons is very nearly equal and the Hall fields for a given current density are rather small. For current along the c axis and a magnetic field in the AB plane, $E_H/E_T \lesssim 1$. Although it is almost impossible to develop a theory which would fully account for all the details for the curves in Fig. 16, approximate calculations of the resistance as a function of the current in thin cylindrical specimens can be made on the basis of the free electron model (see Appendix A). For a fixed value of the current, a fraction of the charge carriers becomes trapped in the magnetic field generated by the current and is unable to collide with the walls. These carriers are then able to travel their full bulk mean free path and their contribution to the current is considerably increased. As the current increases, more and more of the particles are trapped and the resistance steadily decreases as a function of the current. The results of our calculations for three different values of $l_b/2a$ where a is the radius of the wire are shown in Fig. 18.

Although the above calculations are for cylindrical wires, it seems reasonable to assume that the results would not differ qualitatively for a square cross section.

It is clear from Fig. 18 that a theory based upon free electrons cannot explain the increase of resistance with current at large currents observed in gallium wires. This increase of resistance is undoubtedly due to a bulk magnetoresistive effect since the resistance of gallium increases very rapidly if a transverse magnetic field is applied to a specimen carrying current parallel to the C axis (see the previous section, and Reed and Marcus³⁹). The simplest way in which to incorporate a bulk magnetoresistive effect into the simple theory outlined in Appendix A is to require the resistivity of

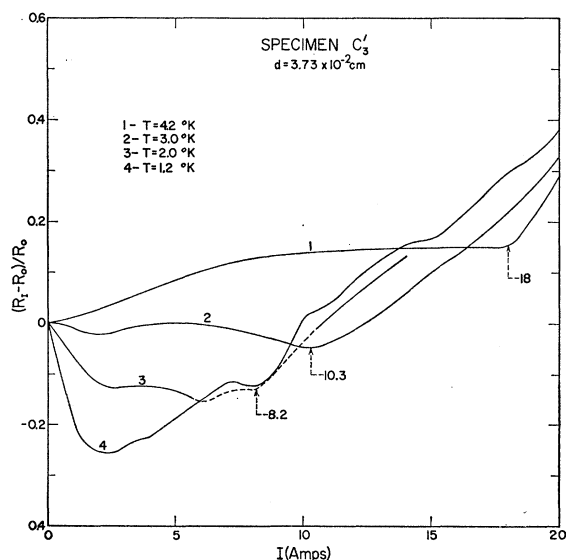


FIG. 17. $\Delta R/R_0$ as a function of the current for the C_3^1 crystal] at different temperatures.

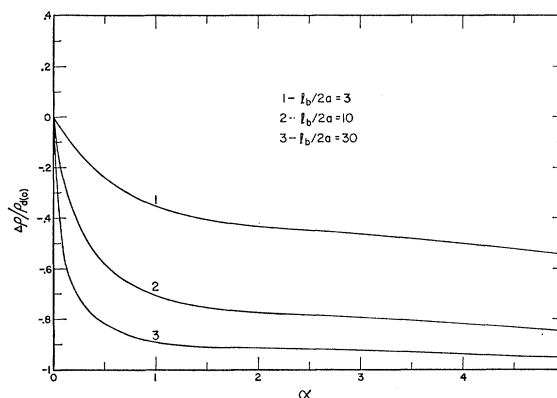


FIG. 18. Calculated values of $\Delta\rho/\rho_a(0)$ for cylindrical wires as a function of $\alpha = aeH_0/mv_0c$, which is directly proportional to the current. l_b is the bulk mean free path and $2a$ is the diameter.

the wire, $\bar{\rho}$, to become the bulk resistivity $\rho_b(H)$ for large currents. From Appendix A, Eq. (A7),

$$\bar{\rho} = \frac{\rho_d(0)}{1 + [(l_b/2a) - 1]F(\alpha)}, \quad (3.9)$$

where $\alpha = (eI/5P_f c) = 0.018 I$, and $F(\alpha)$ is defined by Eq. (A9). The current I is in amperes, and P_f , c , e are, respectively, the momentum of the charge carriers at the Fermi surface of the metal, the velocity of light, and a constant numerically equal to the magnitude of the electronic charge. Since $F(\alpha) \rightarrow 1$ as $\alpha \rightarrow \infty$, we have

$$\lim_{\alpha \rightarrow \infty} \bar{\rho} = \rho_d(0)2a/l_b = \rho_b(0).$$

Consequently, if 3.9 is multiplied by the ratio $\rho_b(H)/\rho_b(0)$, $\bar{\rho}$ will approach the required magnetoresistivity limit for large currents. There is no reason to suppose that this bulk resistivity ratio will be the same as that observed when a uniform transverse field is applied to the specimen; the carriers which contribute to it represent a limited number of states on the Fermi surface. Nevertheless, we have plotted in Fig. 19 the product of 3.9 and a bulk magnetoresistivity function which is similar to experimental curves obtained by applying an external transverse field. The curve so obtained shows a remarkable resemblance to the observed variation of resistance with current for the larger specimens at 4.2°K. Moreover, if the reasonable assumption is made that the bulk magnetoresistance function for current generated fields depends upon the magnetic field and the bulk mean free path of the carriers through the product (Hl_b) , it follows at once that the ratio $\Delta\rho/\rho_d(0)$ depends upon the dimensions of the wire only through the ratio $(l_b/2a)$ in agreement with the observations.

The simple model sketched above cannot explain the additional minima which are apparent in the curves of Figs. 16, 17, and 20. These are presumably due to other carriers having a different Fermi momentum and probably a different mean free path from those carriers

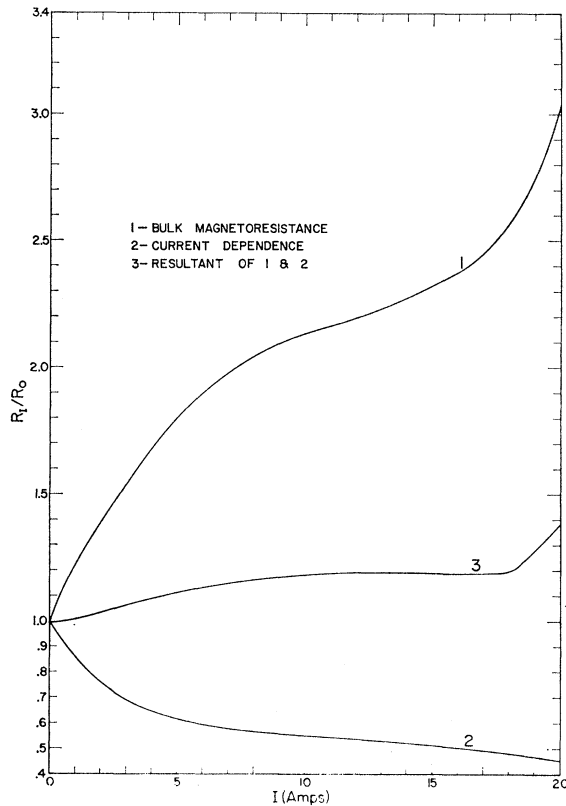


FIG. 19. Graph showing the resultant of the bulk magnetoresistance and the magnetomorphic decrease in resistance as a consequence of the trapping of the charge carriers.

which are responsible for the first minimum. The theory also does not explain the sharp kinks in the resistance current curves at 1.2°K displayed by specimens C_2^2

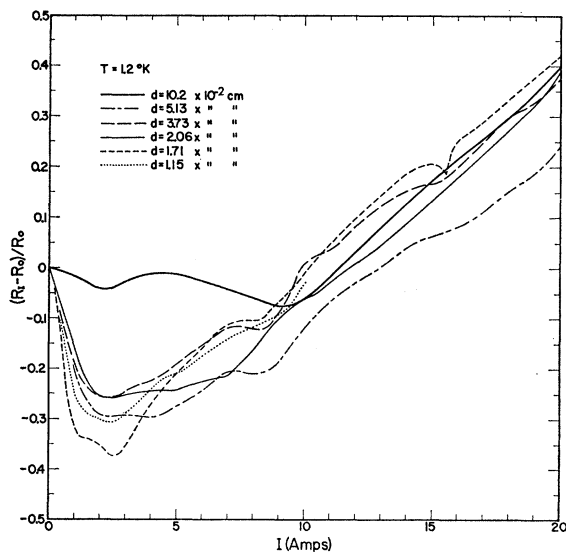


FIG. 20. $\Delta R/R_0$ as a function of the current for the six crystals at 1.2°K.

and C_3^2 . They have been marked by arrows in Fig. 15. For a given specimen, the position and magnitude of these kinks were reproducible to within 0.1%. Apart from the fact that they seem to appear for relatively high current densities, we have not been able to correlate their existence with any other parameter. One notable feature which was associated with them is as follows.

For a given current the potential drop across the specimen was measured by passing the current in the forward and reverse direction and each point in the curves of Fig. 15 represents the mean of the resistance obtained from these two observations. In general, the agreement between the two values of the resistance was better than one percent. However, in the vicinity of these kinks the two values sometimes differed by as much as 3%. Since these anomalies were not found in every crystal, we believe that they may be associated with some unknown defect in a given specimen.

ACKNOWLEDGMENTS

The authors wish to express their thanks to M. Greenebaum for help with the experiments, to Dr. C. A. Shiffman for the permanent loan of his cryostat, to Dr. W. G. Chambers, Professors J. Koringa and C. P. Yang and R. Boughton for helpful discussions.

APPENDIX A: APPROXIMATE CALCULATION OF THE RESISTANCE OF A THIN CYLINDRICAL WIRE AS A FUNCTION OF ITS MEASURING CURRENT

Let H_G be the field due to a uniformly distributed current I A across a cylindrical wire of radius a . At a point P whose distance from the axis of the wire is r , H is of magnitude $H_0 r/a$, where $H_0 = I/5a$, and is directed along the tangent to the circle of cross section through P .

Let r , w , and z denote the cylindrical coordinates for the wire, where the positive z axis is along the axis of the wire in the direction of the current flow. Consider a particle whose position at time $t=0$ is specified by $r=\xi$, $w=0$ and $z=z_0$. Suppose that the particles' velocity vector at $t=0$ is of magnitude v_0 , that it is inclined at an angle Θ to the positive z axis and that its projection in the plane perpendicular to the axis makes angle Φ with the cross-sectional radius. The initial velocity components are then given by

$$v_r = dr/dt = v_0 \sin\Theta \cos\Phi,$$

$$v_w = r dw/dt = v_0 \sin\Theta \sin\Phi,$$

and

$$v_z = dz/dt = v_0 \cos\Theta.$$

We assume that there are no Hall fields acting on the carriers, and neglect the force due to the electric field which causes the current to flow; thus, the force acting on the particle is assumed to be purely magnetic. In a

specimen of diameter 10^{-2} cm $F_E/F_H \approx 10^{-6}$. We also assume henceforth that the particle considered is an electron: the working for a positively charged particle is entirely analogous. Let m denote the mass of the electron and e the absolute value of its charge. Then an integration of Newton's laws of motion, together with initial conditions, gives

$$\frac{1}{2}m(dr/dt)^2 = E_0 - V(r), \quad (\text{A1})$$

where

$$E_0 = \frac{1}{2}mv_0^2 \left\{ \sin^2\Theta - (a/R_0)(\xi/a)^2 \cos\Theta - \frac{1}{4}(a/R_0)^2(\xi/a)^4 \right\} \quad (\text{A2})$$

and

$$V(r) = \frac{mv_0^2}{2} \left\{ \left(\frac{\xi}{a} \right)^2 \frac{\sin^2\Theta \sin^2\Phi}{(r/a)^2} + \frac{1}{4} \left(\frac{a}{R_0} \right)^2 \left(\frac{r}{a} \right)^4 - \left[\left(\frac{a}{R_0} \right) \cos\Theta + \frac{1}{2} \left(\frac{a}{R_0} \right)^2 \left(\frac{\xi}{a} \right)^2 \right] \left(\frac{r}{a} \right)^2 \right\}. \quad (\text{A3})$$

Here $R_0 = mv_0c/eH_0$, is the cyclotron radius of the charge carriers in the maximum field H_0 .

The time taken by the electron to reach the cylinder wall is given by

$$\tau = \int_{\xi}^a \frac{dr}{(dr/dt)} = \int_{\xi}^a \frac{dr}{([\frac{2}{m}][E_0 - V(r)])^{1/2}}. \quad (\text{A4})$$

Let

$$\alpha = a/R_0, \quad x = r/a, \quad \gamma = \xi/a, \quad \epsilon_0 = \frac{E_0}{\frac{1}{2}mv_0^2},$$

and

$$v = \frac{V}{\frac{1}{2}mv_0^2}.$$

Eq. (A4) then becomes

$$\tau = \frac{a}{v_0} \int_{\gamma}^1 \frac{dx}{[\epsilon_0 - v(x)]^{1/2}},$$

where

$$\epsilon_0 = \sin^2\Theta - \alpha\gamma^2 \cos\Theta - \frac{1}{4}\alpha^2\gamma^4$$

and

$$v(x) = (\gamma/x)^2 \sin^2\Theta \sin^2\Phi + \frac{1}{4}\alpha^2x^4 - [\alpha \cos\Theta + \frac{1}{2}\alpha^2\gamma^2]x^2.$$

Now, if $\epsilon_0 - v(x) < 0$ at $x=1$, the particle cannot reach the wall of the cylinder, and in this case its contribution to the current will clearly be much greater.

$$\epsilon_0 - v(1) = -\frac{1}{4}\alpha^2(1-\gamma^2)^2 + \alpha \cos\Theta(1-\gamma^2) + \sin^2\Theta(1-\gamma^2 \sin^2\Phi).$$

Note that $0 \leq \gamma < 1$ and that α depends on the current through the wire.

We see that for any pair of angles Θ and Φ there will be a critical value of the current, such that for any larger current the particle cannot reach the wall. The corresponding critical value of α is given by setting

$\epsilon_0 - v(1) = 0$, which yields

$$\alpha_c = \frac{2}{1-\gamma^2} [\cos\Theta + (1-\gamma^2 \sin^2\Theta \sin^2\Phi)^{1/2}]$$

since we require the positive root.

The particles can now be divided into two groups. The first group contains particles which are "trapped," i.e., which make no wall collisions; this group will be assigned the bulk mean free path l_b . The second consists of "untrapped" particles, which collide with the walls; we shall assume that these have an effective mean free path $2a$. It is of course assumed that $l_b/2a \gg 1$.

Since the expression for α_c is not very sensitive to Φ , we shall assume for simplicity that $\Phi=0$. In this case, given a value of the current, or equivalently given a value of α , we can define a critical angle Θ_c , where

$$\Theta_c = \cos^{-1} \left\{ \frac{1}{2}(1-\gamma^2)\alpha - 1 \right\}$$

such that for all Θ with $\Theta_c \leq \Theta \leq \pi$, the electrons are trapped and have a mean free path l_b .

The conductivity at the point $\xi = \gamma a$ is given by the Chambers tube integral⁷

$$\sigma(\xi) = \frac{3 ne^2}{2 mv_0} \int_0^\pi l_{\text{eff}} \sin\Theta \cos^2\Theta d\Theta. \quad (\text{A5})$$

Here again an approximation has been made. We assume that the energy gained by the particles from the electric field is not affected by the spiralling of the charge carriers round the magnetic lines of force and that $\Delta E = el_{\text{eff}} \cos\Theta \times$ (electric field). The assumption is crude but should not affect the results qualitatively.

Substituting the value of l_{eff} from above we have

$$\begin{aligned} \sigma(\xi) &= \frac{3 ne^2}{2 mv_0} \left\{ \int_0^{\Theta_c} 2a \sin\Theta \cos^2\Theta d\Theta + \int_{\Theta_c}^\pi l_b \sin\Theta \cos^2\Theta d\Theta \right\} \\ &= \frac{ne^2 a}{mv_0} \left\{ 1 - \cos^3\Theta_c + \frac{l_b}{2a} (1 + \cos^3\Theta_c) \right\}. \quad (\text{A6}) \end{aligned}$$

As $\alpha \rightarrow 0$, $\Theta_c \rightarrow \pi$ and $\sigma(\xi) \rightarrow \sigma_d(0)$, where $\sigma_d(0) = (ne^2/mv_0)(2a)$ is the conductivity of the wire extrapolated to zero current.

Thus

$$\begin{aligned} \sigma(\xi) &= \frac{\sigma_d(0)}{2} \left\{ \left(1 + \frac{l_b}{2a} \right) + \left(\frac{l_b}{2a} - 1 \right) \right. \\ &\quad \left. \times \left[\frac{\alpha^3}{8} (1-\gamma^2)^3 - \frac{3\alpha^2}{4} (1-\gamma^2)^2 + \frac{3}{2}\alpha (1-\gamma^2) - 1 \right] \right\} \end{aligned}$$

since $\cos\Theta_c = \frac{1}{2}(1-\gamma^2)\alpha - 1$. The average conductivity, $\bar{\sigma}$, must be obtained by taking the average of $\sigma(\xi)$

across the section of the wire. Thus

$$\begin{aligned}\bar{\sigma} &= \frac{1}{\pi a^2} \int_0^a 2\pi\sigma(\xi)\xi d\xi, \\ &= 2 \int_0^1 \sigma(\gamma)\gamma d\gamma, \\ &= \int_0^1 \sigma(x)dx, \quad \text{where } x=1-\gamma^2.\end{aligned}$$

For any given α , all particles are trapped if $x=(1-\gamma^2) \geq 4/\alpha$. In this case the conductivity is just the bulk conductivity $\sigma_b = \sigma_d(0)[l_b/2a]$.

On evaluating the integrals for $\bar{\sigma}$, we have

$$\bar{\sigma} = \sigma_d(0) \left\{ 1 + \left[\frac{l_b}{2a} - 1 \right] \times \alpha \frac{1}{64} (\alpha^2 - 8\alpha + 24) \right\}, \quad \text{if } 0 \leq \alpha < 4$$

or

$$\bar{\sigma} = \sigma_d(0) \left\{ 1 + \left[\frac{l_b}{2a} - 1 \right] \left[1 - (2/\alpha) \right] \right\}, \quad \text{if } \alpha \geq 4. \quad (\text{A7})$$

(The second integral is evaluated in two pieces.) With $\bar{\rho} = 1/\bar{\rho}$, $\sigma_d(0) = 1/\rho_d(0)$, we obtain

$$\frac{\bar{\rho} - \rho_d(0)}{\rho_d(0)} = \frac{-\left[\frac{l_b}{2a} - 1 \right] F(\alpha)}{1 + \left[\frac{l_b}{2a} - 1 \right] F(\alpha)}, \quad (\text{A8})$$

where

$$\begin{aligned}F(\alpha) &= (\alpha/64)(\alpha^2 - 8\alpha + 24) \quad \text{if } 0 \leq \alpha < 4 \\ &= [1 - (2/\alpha)] \quad \text{if } \alpha > 4.\end{aligned} \quad (\text{A9})$$

APPENDIX B. SOME RELEVANT PROPERTIES OF GALLIUM

Resistivities for current flow along the principle axes^{20,23} are shown in Table IV.

TABLE IV. Resistivities for current flow along the principle axes.

Axis	$T=20^\circ\text{C}$ ($\Omega\text{-cm}$)	$T=0^\circ\text{C}$ ($\Omega\text{-cm}$)	$T=-195.8^\circ\text{C}$ $= 77.4^\circ\text{K}$ ($\Omega\text{-cm}$)
A	17.27×10^{-6}	15.8×10^{-6}	3.04×10^{-6}
B	7.85×10^{-6}	7.17×10^{-6}	1.42×10^{-6}
C	55.53×10^{-6}	51.3×10^{-6}	10.5×10^{-6}

Gallium has an orthorhombic cell containing 8 atoms³⁵ with lattice constants⁴² at $T=2.35^\circ\text{K}$, $A=4.5151 \text{ \AA}$, $B=4.4881 \text{ \AA}$, $C=7.6318 \text{ \AA}$. The volume of the orthorhombic cell is $V_0 = ABC = 1.547 \times 10^{-22} \text{ cc}$. Each gallium atom has three valence electrons outside a closed $3d$ shell: the number of valence electrons per unit volume at 2.35°K is

$$N = 24/V_0 = 1.551 \times 10^{23}.$$

Volume of gallium per gram atom at $2.35^\circ\text{K} = 11.65 \text{ cc}$, density¹⁹ at $20^\circ\text{C} = 5.907 \text{ g/cc}$, and density at $2.35^\circ\text{K} = 5.983 \text{ g/cc}$.

Properties of a free-electron gas having the same electron density as gallium. Momentum of an electron having the Fermi energy:

$$P_f = 1.752 \times 10^{-19} \text{ cgs.}$$

The wavelength of an electron having the Fermi momentum

$$\lambda_f = h/P_f = 3.780 \times 10^{-8} \text{ cm.}$$

The Fermi energy: $E_f = P_f^2/2M_0 = 16.85 \times 10^{-12} \text{ ergs} = 10.52 \text{ eV}$. The cyclotron radius of an electron having the Fermi energy:

$$r_0 = P_f c/eH = 10.94/H \text{ cm, } H \text{ is in gauss.}$$

⁴² C. S. Barrett, in *Advances in X-ray Analysis*, edited by W. M. Mueller (Plenum Press, New York, 1962), Vol. 5.

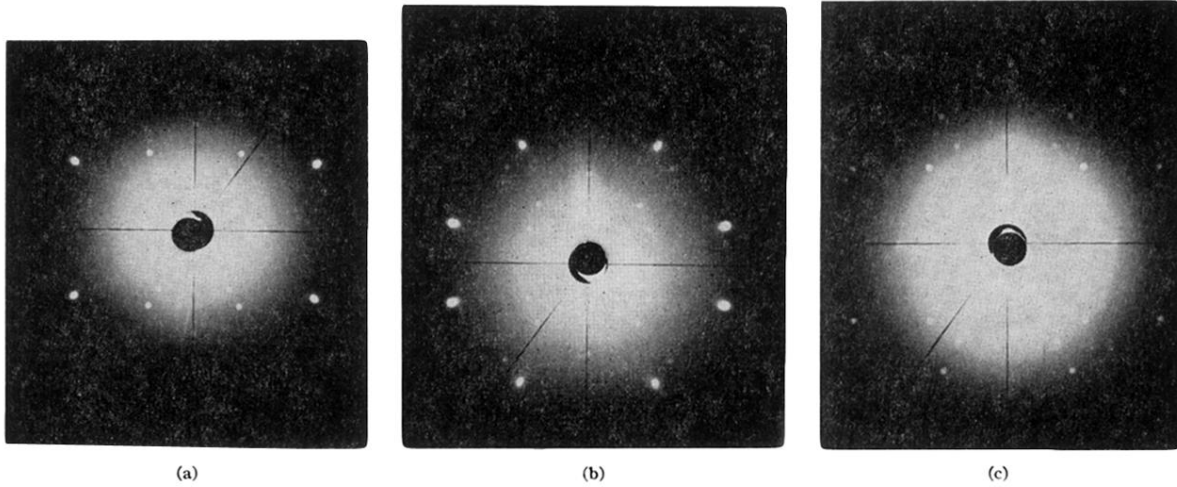


FIG. 2. Laue back reflection photographs of three oriented crystals. (a) Incident x-ray beam parallel to the A axis. (b) Incident x-ray beam parallel to the B axis. (c) Incident x-ray beam parallel to the C axis.